Available online at www.sciencedirect.com
ScienceDirect
Physica E 40 (2008) 1305–1308
PHYSICA E
www.elsevier.com/locate/physe

Mechanical buckling of multi-walled carbon nanotubes: The effects of slenderness ratio

Jian-Ming Lu[a,b], Chi-Chuang Hwang[a,*], Qu-Yuan Kuo[c], Yun-Che Wang[c,d,**]

[a]*Department of Engineering Science, National Cheng Kung University, Tainan, Taiwan 70101, Taiwan*
[b]*National Center for High-Performance Computing, National Applied Research Laboratories, No. 28, Nanke 3rd Rd., Sinshih Township, Tainan, Taiwan 71447, Taiwan*
[c]*Materials Program, Department of Civil Engineering, National Cheng Kung University, Tainan, Taiwan 70101, Taiwan*
[d]*Center for Micro/Nano Science and Technology, National Cheng Kung University, Tainan, Taiwan 70101, Taiwan*

Available online 18 September 2007

Abstract

Buckling strengths, in terms of compressive strain, of single-, double- and triple-walled carbon nanotubes (CNTs) are investigated to study the effects of slenderness ratio (S_R) via the molecular dynamics (MD) simulations with the Tersoff potential. Under constant ratio of slenderness, the CNTs with small S_R behave like a continuum shell object. For large S_R's, multi-walled CNTs exhibit the characteristics of the Euler columns. In addition, smaller nanotubes possess higher buckling-resistance. The buckling strength of multi-walled nanotubes is controlled by the size of their outermost shell.

PACS: 62.25.+g; 81.07.De; 82.20.Wt

Keywords: Carbon nanotube; Buckling; Molecular dynamics simulation

1. Introduction

Since the discovery of carbon nanotubes about 15 years ago [1], research in the mechanics of carbon nanotubes (CNTs) and their buckling behavior has been intensive. The buckling behavior of the nanotubes is usually utilized as a probe to characterize their mechanical properties. For example, from molecular dynamics (MD) simulation of the mechanical properties of the nanotubes, the Young's modulus and Poisson's ratio of a single-walled carbon nanotubes (SWCNTs) are found to be 5.5 TPa and 0.19, respectively [2]. Recent MD simulation studies on variations of Young's modulus of SWCNTs can be found in [3]. Note that Young's modulus of SWCNTs has been determined via thermal-noise vibrational experiments to be about 1.8 TPa [4]. Experimentally, nanoindentation tests on vertically aligned carbon nanotubes have shown the Young's modulus of the nanotube's wall to be on the order of 5 TPa, and the Young's modulus obtained from bending and axial deformation is on the order of 1 TPa [5]. In the literature, there are also many MD simulation results on multi-walled nanotubes. For example, Sears and Batra [6] study the buckling of double-walled carbon nanotubes (DWCNTs) and three-walled carbon nanotubes (TWCNTs) with continuum finite element truss models and MD simulations with the MM3 interatomic potential. Liew et al. [7] studied four-walled carbon nanotubes with the Brenner potential [8]. All of these research did not study the effects of slenderness ratio on the buckling behavior of the nanotubes.

In this paper, we perform MD simulation to study the buckling behavior of single- and multi-walled carbon nanotubes under unaxial compressive displacement loading. Several nanotubes are studied here, including the (3, 3), (5, 5), (10, 10), and (15, 15) SWCNTs; (5, 5)@(10, 10) and (10, 10)@(15, 15) DWCNTs; and (5, 5)@(10, 10)@(15, 15)

*Corresponding author.
**Also for correspondance. Center for Micro/Nano Science and Technology, National Cheng Kung University, Tainan, Taiwan 70101, Taiwan. Tel.: +886 6 2757575 63140; fax: +886 6 235 8542.
E-mail addresses: chchwang@mail.ncku.edu.tw (C.-C. Hwang), yunche@mail.ncku.edu.tw (Y.-C. Wang).

1386-9477/$ - see front matter © 2007 Elsevier B.V. All rights reserved.
doi:10.1016/j.physe.2007.08.120

triple-walled carbon nanotube (TWCNT). After calculating the strain energy density of the nanotubes with various slenderness ratio (defined later), we perform a correlation study to identify the effects of slenderness ratio on buckling strain. Further, we discuss the changes in buckling modes as a result of changes in the relationship between the nanotubes' lengths and slenderness ratios.

2. Simulation

The mechanical problem of the buckling of the single- or multi-walled carbon nanotube is depicted in Fig. 1. The carbon nanotube has a diameter of D, twice of its radius (R), and unconstrained length L_u. On both the top and bottom of the tube, there are four atomic layers of carbon fixed to simulate the clamped–clamped boundary condition in the context of continuum mechanics. The compression process is performed through moving the displacement of the top end downwards. The bottom end is held fixed throughout simulation. We adopted a displacement rate of 10^{-12} nm/fs downwards, and define the unconstrained length (L_u) of the nanotubes to be the total length (L) minus the fixed lengths.

Similar to the standard notation, $C_h = na_1 + ma_2$, in the literature to describe the chirality of the nanotube, we define base vectors $b_1 = a_1 + a_2$ and $b_2 = a_1 - a_2$, which are suitable for the armchair-type carbon nanotubes to facilitate our definition of the slenderness ratio. Analogously, we further define $C = Nb_1 + Mb_2$, and thus the slenderness ratio can be defined as $S_R = N/M$, which is

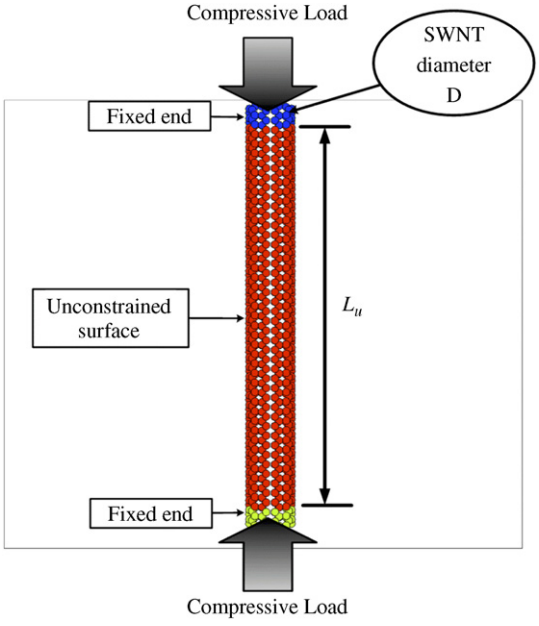

Fig. 1. Schematic of the carbon nanotube under compression via displacement control at the top end. The bottom end is held fixed throughout simulation. On either the top or bottom end, four atomic layers of carbon are held fixed to simulate the clamped-clamped boundary condition. The carbon nanotube has a diameter of D, twice of its radius (R), and unconstrained length L_u.

proportional to the radius-to-length ratio ($\lambda = R/Lu$). To get a sense of the relationship between the slenderness and radius-to-length ratios, we note that $S_R = 1$ translates to $\lambda = 0.276$. Note that the diameter of a carbon nanotube can be computed as $D^2 = 3a^2(m^2 + n^2 + mn)/\pi^2$, where (m, n) is the chirality of the carbon nanotube and the symbol $a = 1.44$ denotes the interatomic C–C bond length. Here we perform MD calculations to obtain the relationship between strain energy density and applied compressive strain for the SWCNTs (3, 3), (5, 5), (10, 10), (15, 15), DWCNTs (5, 5) (10, 10), (10, 10)@(15, 15), and a TWCNT (5, 5)@(10, 10)@(15, 15). Buckling strains (or called critical strains) can be inferred from the jumps in the strain energy density.

The empirical Tersoff potential [9–11] was employed to derive the interatomic forces among the carbon atoms of the CNTs. This particular potential model is chosen since it provides quick estimates and significant insights into the thermo-mechanical behavior of the nanotubes without the need to consider chemical reactions. The motion of each carbon atom was governed by Newton's laws of motion, in which the resultant force acting on each atom was deduced from the energy potential related to its interactions with neighboring atoms within a prescribed cut-off radius. The conventional Leap-Frog algorithm [12] was employed to derive the new position and velocity of each atom based on the data obtained in the previous step. Our simulation time step was $\Delta t = 1$ fs, and an equilibrium configuration was searched with a verlet list. Further, the nanotube was maintained at the specified temperature (1 K throughout) using a rescaling method [13]. The effects of boundary constraints have been shown insignificant in affecting buckling strains, provided with the buckling kinks form near the middle along the nanotubes length.

3. Results and discussion

The radii of the (3, 3), (5, 5), (10, 10) and (15, 15) carbon nanotubes are 0.206, 0.344, 0.688 and 1.031 nm, respectively. For $S_R = 1$, their corresponding unconstrained lengths (L_u) are 0.748, 1.247, 2.494 and 3.741 nm, and the numbers of atom in L_u are 42, 110, 420 and 930. The DWCNT or TWCNT are the combination of the four types of SWCNTs. As for using the Tersoff potential to simulate carbon nanotubes, we remark that due to the assumptions in the Tersoff potential, simulation results at large strains may not be reliable and will not be shown in the present analysis. Although the quantitative validity of the Tersoff potential in large strains can be examined by a comparative study with ab initio calculations, it is conceivable that the Tersoff potential is suitable for buckling studies up to the first buckling mode discussed here.

The relationship between buckling strain and the slenderness ratio is shown in Fig. 2 for all the carbon nanotubes studied here. It can be seen that the effects of the slenderness ratio diminishes as the radius of the CNTs

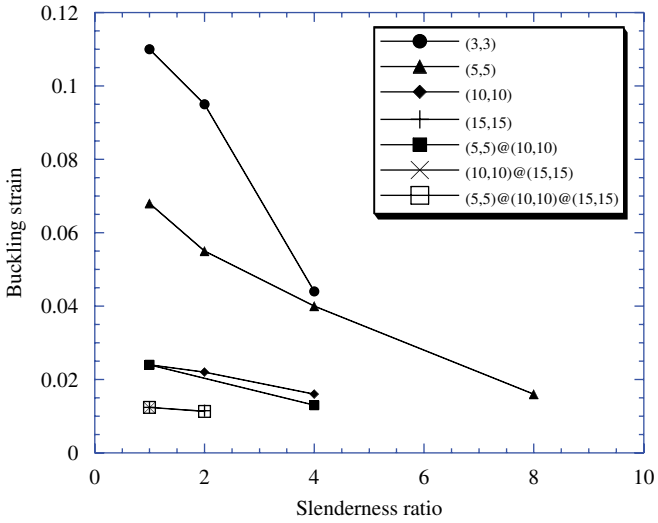

Fig. 2. Buckling strain vs. slenderness ratio for different armchair types of single-walled and multi-walled CNTs. The effects of the slenderness ratio diminishes as the radius of the CNTs increases. There is only one data point for the (10,10)@(15,15) DWCNT. For small-radius CNTs, changes in the slenderness ratio imply changes in buckling modes from local kink formation to globally lateral buckling.

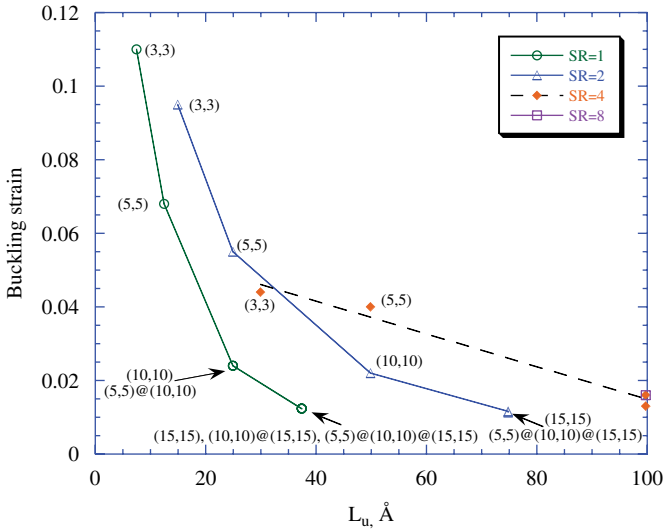

Fig. 3. Buckling strain vs. unconstrained length (L_u) under a specified slenderness ratio. Labels show overlapped data points from different CNTs. For example, the (10,10) single-walled CNT shares the same buckling strain as the (5, 5)@(10, 10) double-walled one. Comparisons between single- and multi-walled CNTs show that the size of the outer shell of the tube determines its buckling strength. When S_R equals to 1 or 2, the trend of buckling strain vs. unconstrained length is typical for cylindrical shells in the context of continuum elasticity. For large S_R's, the trend is close to that of the buckling of the Euler solid column, indicating changes in buckling modes. At $L_u = 100$, the lower diamond indicates the ε_{cr} for the (5, 5)@(10, 10) DWCNT, and the upper one is for the (10,10) SWCNT. The open square is obtained from the (5,5) SWCNT.

increases, indicating changes in buckling modes. For small S_R, the nanotubes are short, and their buckling is dominated by local kink formation. For large S_R, global buckling is favorable, and deformation mode is lateral bending. For DWCNT or TWCNTs, their buckling strain is the same as their outer shell alone. For example, the (10,10) SWCNT has similar buckling strength as the (5, 5)@(10, 10) DWCNT, and (15, 15), (10, 10)@(15, 15) and (5, 5)(10, 10)(15, 15) show the same buckling strain for $S_R = 1$. Therefore, for multi-walled carbon nanotubes, the inner shells do not increase the overall buckling strain of the cylindrically composited tubes. There is a small difference between the (10, 10) SWCNT and (5, 5)@(10, 10) DWCNT.

Under a specified S_R, we show buckling strain in terms of unconstrained length in Fig. 3. Note that since S_R is fixed for a specific case, different L_u indicates different tube radius. Labels show which type of the CNTs that the data points belong to. For example, the (10, 10) SWCNT shares the same buckling strain as the (5, 5)@(10, 10) double-walled one. More, the (15, 15) SWCNT, (10, 10)@(15, 15) DWCNT and (5, 5)@(10, 10)@(15, 15) TWCNT exhibit the same buckling strength, confirming the results from the study of the effects of S_R in Fig. 2. In other words, multi-walled CNTs show that the size of the outer shell of the tube determines its buckling strength. When $S_R = 1$ or 2, the trend of buckling strain vs. unconstrained length is typical for cylindrical shells in the context of continuum elasticity [14]. For large S_R's, due to changes in buckling modes from local to global, the trend of the relationship between buckling strain and L_u is close to that of the buckling of the Euler solid column, which predicts different L_u's correspond to the same buckling strain. The slope of the linear curve fit among the solid diamonds (i.e. the dashed line) is -4.45×10^{-4} Å^{-1}, indicating the nanotubes' behavior approaches that of a solid column. At $L_u = 100$, there are three data points, indicating the outermost shell of multi-walled CNTs dominate their buckling strain.

4. Conclusions

Based on the results of our MD simulation, smaller nanotubes have higher buckling resistance. Moreover, the buckling strength of carbon nanotubes increases when the size of tubes decreases for small S_R. This phenomenon is a direct result of changes in buckling modes from local to global buckling. For small S_R's, smaller CNTs exhibit steep reduction in buckling strength with respect to L_u. However, for large S_R's, the buckling strain tends to be independent on L_u. This change in the relationship between buckling strain and unconstrained length is due to changes in buckling modes. Nanotubes with large S_R behave more like the Euler column. For multi-walled nanotubes, their buckling strength is dominated by the size of their outermost shell.

Acknowledgments

The authors acknowledge a grant from the Taiwan National Science Council under the Contract NSC 94-2515-S-006-010.

References

[1] S. Iijima, Nature 354 (1991) 56.
[2] B.I. Yakobson, C.J. Brabec, J. Bernholc, Phys. Rev. Lett. 76 (14) (1996) 2511.
[3] J.Y. Hsieh, J.M. Lu, M.Y. Huang, C.C. Hwang, Nanotechnology 17 (2006) 3920.
[4] M.M.J. Treacy, T.W. Ebbesen, J.M. Gibson, Nature 381 (1996) 678.
[5] H.J. Qi, K.B.K. Teo, K.K.S. Lau, M.C. Boyce, W.I. Milne, J. Robertson, K.K. Gleason, J. Mech. Phys. Solids 51 (2003) 2213.
[6] A. Sears, R.C. Batra, Phys. Rev. B 73 (2006) 085410.
[7] K.M. Liew, C.H. Wong, X.Q. He, M.J. Tan, S.A. Meguid, Phys. Rev. B 69 (2004) 115429.
[8] D.W. Brenner, Phys. Rev. B 42 (15) (1990) 9458.
[9] J. Tersoff, Phys. Rev. Lett. 56 (1986) 632.
[10] J. Tersoff, Phys. Rev. B 37 (1988) 6991.
[11] J. Tersoff, Phys. Rev. B 39 (1989) 5566.
[12] M.P. Allen, D.J. Tildesley, Computer Simulation of Liquids, Oxford Science Publications, Oxford, UK, 1987.
[13] D.C. Rapaport, The Art of Molecular Dynamics Simulation, Cambridge University Press, London, UK, 1997.
[14] T. von Karman, H. Tsien, J. Aeronaut. Sci. 8 (1941) 303.